

DESIGNING QUAD BUNDLES AGAINST GALLOPING

- by -

A.S. Richardson, Jr.

Research Consulting Associates
Lexington, Massachusetts, USA

Presentation at the AIM Study Day on Galloping

University of Liège
10 March 1989

DESIGNING QUAD BUNDLES AGAINST GALLOPING

by: A.S. Richardson, Jr.
Research Consulting Associates
Lexington, Massachusetts, USA

ABSTRACT:

The paper addresses the issue of galloping in quad-bundled transmission lines. Recent experiences with galloping of quad-bundled lines in the U.K. are used as a point of departure for the study. Aerodynamic data obtained from wind tunnel studies in England are compared to wind tunnel data obtained 25 years ago under an M.I.T. study. The former data were obtained from models designed from actual ice forms responsible for the quad-bundle gallop. The latter data were obtained from smooth models having simulated tear drop ice shapes. After adjusting for differences in Reynolds number, the two sets of data compare within about 10% over a range of angle of attack from minus to plus 40 degrees.

Analytical studies start from the linear equations of motion in two degrees of freedom, gallop and twisting. The wind tunnel data are approximated by analytical curves. The critical wind speed of gallop is found to depend on damping factor in both modes, mass radius of gyration of the bundle, mass unbalance, and especially, on initial angle of attack. The phase of the twist motion is in phase with the gallop velocity, and the magnitude of the twist motion always exceeds the magnitude of the angle of attack due to gallop. The linear studies are followed by non-linear studies which illustrate the build up of gallop amplitude once the critical wind speed is reached. The effects of the mass radius of gyration, the mode damping, and the initial angle of attack are similar to the linear studies.

INTRODUCTION

From the earliest times of concern for the 'gallop problem' there has been controversy and disagreement. A consensus has never been agreed to by the serious researchers of any given period. An example may be found in the proceedings of a conference on galloping conductors, (1948). Attending that conference were A.E. Davidson, W.F. Dobson, A.T. Edwards, J.H. Waghorne, and others from Ontario Hydro. Also in attendance were, J.P. Den Hartog, R.T. Henry, M.S. Oldacre and others from the United States. And, since the conference was held at the National Research Council of Canada, several from that institution attended such as F. Cheers, R.J. Templin, and R. Ruedy.

A considerable discussion centered around the issue of the lift curve slope. Professor Den Hartog expressed his famous view that the negative slope was a primary factor in the gallop problem, while Dr. Ruedy felt that the positive slope region was the dominant influence. With some minor modifications, the argument continues today.

While this paper does not presume to settle the issue, the perception that this author has is this: Negative slope regions of the lift curve are in the usual sense of Den Hartog Galloping responsible for galloping of both single and bundled cables in light ice. In heavy ice, galloping is mostly due to the positive lift curve slope in combination with a coupling of the gallop motion with cable twisting. In the former case, some twisting may appear, but it is not essential to the instability. Rather it is incidental to it. In the latter case the coupling of the torsion with the gallop is most essential, and it is easily accomplished when the natural frequencies of gallop and torsion are in close proximity. Further, in the latter case, coupling is primarily aerodynamic as opposed to inertial. In the former case, coupling could be either, or both.

This paper examines the second kind of gallop. For simplicity, the natural frequencies are considered almost equal. The stability of a cable span is examined by both linear and non-linear methods. The linear methods are put into the same general form of Nakamura (1980). The non-linear methods are put into the form of Richardson (1988). The basis of the numerical analysis is a system of bundled spans in the U.K. that have been troubled in recent years by galloping, Tunstall (1987).

Important parameters identified by the linear analysis are confirmed as being important in the non-linear analysis. Certain aspects of the analysis can be interpreted in terms of currently used anti-gallop measures.

Aerodynamic Data

There is no doubt that aerodynamic lift is the primary cause of galloping. While some may debate the slope of the lift curve in relation to the angle of attack, none will question the role of the lift itself in galloping. One needs only to examine the energy input to the motion of gallop. For gallop to grow lift must act in the same direction as the moving cable. Thus, one needs to establish the relation between cable motion, angle of attack, and lift. Drag is important also, because in the classic Den Hartog gallop it alone cancels the effect of negative-going lift with angle of attack. Drag is important in the non-linear analysis of galloping. It sets the final amplitude in the Den Hartog type of gallop, Richardson (1988). The simplicity of the single-degree-of-freedom gallop is lost when only one other degree of freedom is added, such as twisting. Other parameters come into play. Here, we will make the analysis around a fixed set of aerodynamic data. The data are replicated by wind tunnel tests on an 'actual ice shape', Koutselous (1988). The data are seen in Figs. (1), (2), and (3).

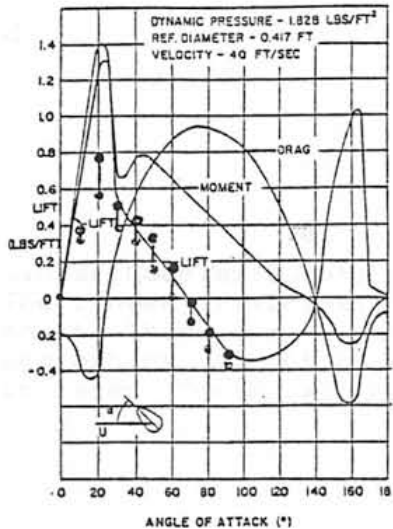


FIG. 1

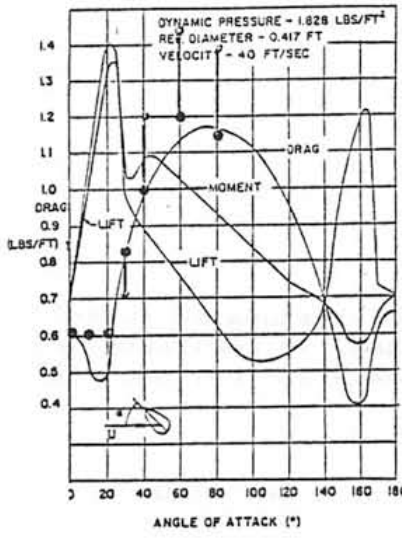


FIG. 2

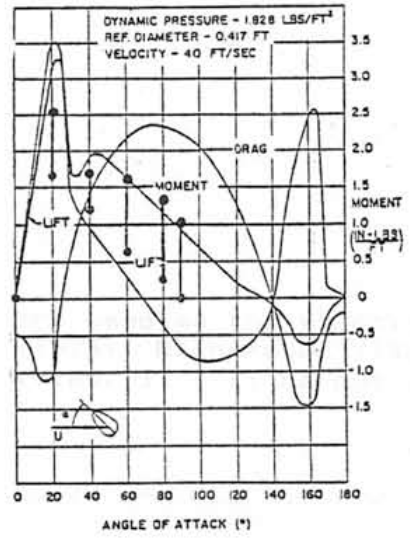


FIG. 3

The data are shown in comparison to data obtained in 1960, and reported later by Richardson (1965). The two shapes are similar. The major difference is in the Reynolds numbers of the tests. In the earlier tests a Reynolds number of about 100,000 was used. In the recent tests the Reynolds number was in the range of about 15,000 to 33,000. In Fig. (1) we see the lift data. The solid curves are from the earlier tests. The max/min range of the recent tests are indicated by the connected closed circles. In comparing the two, the higher values of the closed circles should be favored for lift and pitching moment, while the lower values of the closed circles should be favored for drag. That is, the Reynolds number of 33,000 is thus favored. As seen in Figs. (2) and (3), the agreement is good. One argument used in recent years has been that wind tunnel data taken on smooth surface models, is not applicable to actual iced conductor shapes. Here we have conclusive evidence to the contrary.

It is often convenient to fit analytical curves to the test data for the purpose of analysis and study of parameters. In this case the test data of vintage are fitted, as follows:

Lift: $CL = 0.65 \sin(\pi a) \dots \dots \dots (1)$

Normal Force: $CN = 1.6 \sin(\pi a/2) \dots \dots \dots (2)$

Moment: $CM = 0.7 \sin(1.15 \pi a) \dots \dots \dots (3)$
 If: $a \leq 0.666$

or: $CM = 0.4 \sin(\pi a/2)$
 If: $a > 0.666$

Linear Coupled Equations:

The linear differential equations of Nakamura (1980) are used as the starting point. These are the same as the equations of Chadha (1974), Richardson (1965), and others, except that inertial coupling has been omitted. It will be put back in later. The equations are:

$$y'' + gy' + y = 1/2 q d U^2 (1/mw^2) [-Cna wy'/U + CLa Q] \dots\dots (1)$$

$$Q'' + RgQ' + R^2 Q = 1/2 q d^2 U^2 (1/Iw^2) [-Cma wy'/U + Cma Q] \dots\dots (2)$$

where,

- y = gallop amplitude
- Q = pitch amplitude
- d = cable diameter
- g = loss factor (structural damping)
- U = wind speed normal to cable
- q = density of the air @ 0 deg.C
- m = cable mass per unit length
- I = mass moment of inertia per unit length
- R = pitch frequency/gallop frequency
- w = frequency of the gallop mode (rad/s)
- CNa = slope of normal force coefficient
- CLa = slope of lift force coefficient
- Cma = slope of moment coefficient
- ' , '' = differentiation on wt
- t = time (sec.)

These equations are applicable to a continuous span if the mode shape of the pitch motion (twisting) is the same as the mode shape of the gallop motion. This was pointed out by Richardson and Martucelli in 1963. Further, in a linear system there will be no coupling between first and second modes. That is simply a consequence of the orthogonal relationship between modes. The latter statement does not apply when motions are large, and forces are non-linear. A solution of the coupled equations is to be found from the following matrix equation, after assuming simple harmonic motion at frequency, w:

$$\begin{bmatrix} [\mu g + U_0 CD] i & 0 \\ 0 & \mu r_a R [g i + (R - \frac{1}{R})] \end{bmatrix} \begin{bmatrix} Ar \\ Q \end{bmatrix} = U_0 \begin{bmatrix} -CLa i & CLa \\ -U_0 Cma i & U_0 Cma \end{bmatrix} \begin{bmatrix} Ar \\ Q \end{bmatrix} \dots\dots (3)$$

where,

- μ = $m / (1/2 q d^2)$ relative density
- r_a = dimensionless radius of gyration (squared)
- U_0 = $U / (wd)$, reduced wind speed
- i = $\sqrt{-1}$
- CD = drag coefficient
- Ar = reduced amplitude, scalar, ($=wY/U$)
- Q = vector pitch amplitude, (Magnitude= Q_0)

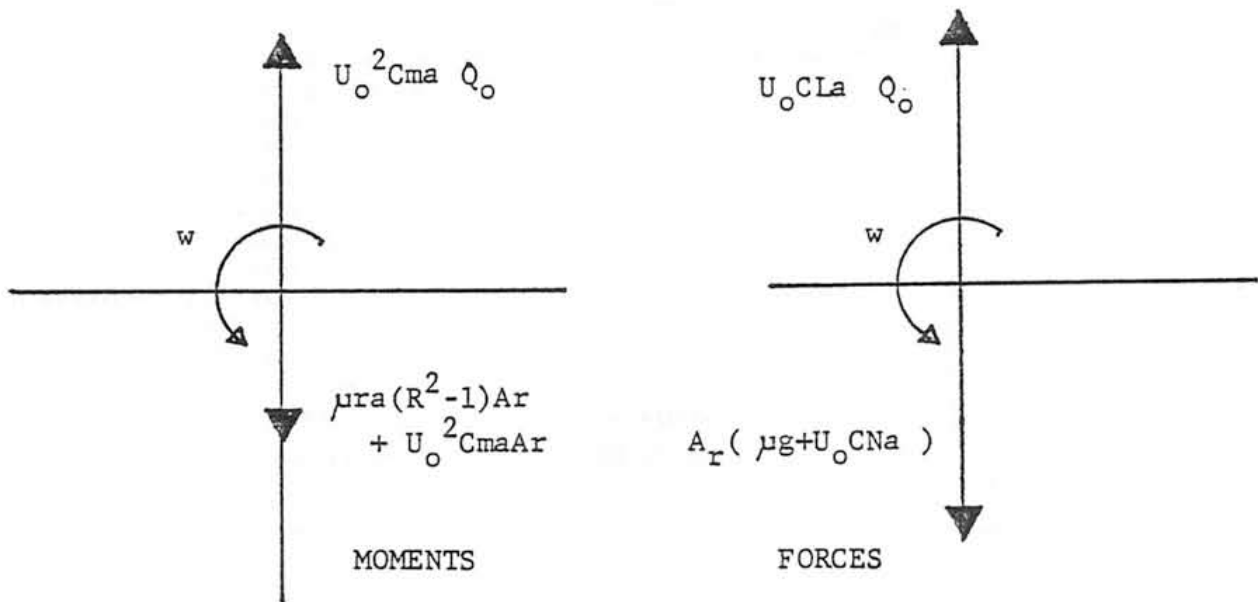


Fig. (7) Orientation of Vectors
Pitch Damping = 0

Reference may be made to Fig.(7) to see the orientation of the vectors. Notice that $Q_0 > A_r$ is a condition for gallop when $CLa > 0$ AND $R \neq 1$. The careful reader will verify that this condition must be satisfied if the energy flow from the wind to the conductor is positive. Clearly, this is a consequence of fundamental mechanical principles. On the other hand, when $CLa < 0$, then the condition, $Q_0 < A_r$ applies. In general, Q_0 may be interpreted as the magnitude of the vector of Q that is in phase with the velocity of the gallop. When the dynamic analyses are considered, the phasor diagram may be used to obtain motion magnitude, phase, and other information. In general, the linear problem involves a separation of variables into real and imaginary parts, and an iterative process that leads to relations between damping (g), and reduced wind speed U_0 . Many hundred solutions of the parameterized system were reported in an earlier study, Richardson, (1965).

The solution of the linear eigenvalue problem is found from the determinant expression,

$$\begin{vmatrix} (G + CLa)i & -CLa \\ Cma i & H^* - Cma \end{vmatrix} = 0 \dots\dots\dots (4)$$

where,

$$G = (\mu g / U_0) + CD$$

$$H^* = R(\mu g ra / U_0^2)i - \mu(1-R^2)ra / U_0^2$$

It is noted that all of the above equations follows closely the derivation of Richardson and Martuccelli (1965). Also, in that study, it was proven that the analysis, though seemingly restricted to a lumped parameter model, does in fact apply to a continuous span, having distributed properties.

The parameters for the subconductor are seen in Table 1.

TABLE 1 Properties of C.E.G.B. Conductor

Item	Numerical Value
Configuration	Quad = 4 (square)
Span	355m
Spacers	0.305m and 0.508m
Conductor diameter	28.6mm (400mm ²)
Conductor strands	54/7 ACSR
Sag @ 0deg.C	10m
Natural Frequencies:	
1st mode gallop	0.169 Hz
1st mode torsion	0.244 Hz
2nd mode gallop	0.349 Hz
2nd mode torsion	0.365 Hz
(calculated frequencies are with no ice or wind)	
Ice Shape	
Model no. 2 (Tunstall & Koutselos)	
Mass of ice	0.3 kg/m
Total mass	2 kg/m
Conductor Tension (no ice)	28.2 kN
C.G. offset (%)	7

A study of Equ.(4) for the parameters of the CEGB cable indicates that the transfer function, Q_0/A_r , is of order unity with phase zero. In other words, a pitch angle driven by the reduced angle of attack, $-A_r$, is in phase with the gallop VELOCITY. Indeed, an examination of vector phasor diagrams indicates that pitch angle magnitude, Q_0 , must be greater than A_r when the frequency ratio $R \sim 1$. Otherwise energy will not flow into the gallop motion from the aerodynamic lift force. Drag force always soaks up energy, as may be seen from the left hand side of Eq.(3), where it adds algebraically to the loss factor μg in proportion to wind speed. Earlier solutions of the equations; also included a 10% offset C.G., and an initial angle of attack of plus or minus 70 degrees. These are reproduced in Fig.(8). Notice that the plot of wind speed is referred to the pitching (torsion) frequency, which also includes a ratio $R=1$. Also, notice the effect that large increases in radius of gyration has; namely, it INCREASES the stability. However, when the frequency ratio, R is near unity the stability is decreased. The damping shown in Fig.(8) is the damping required to satisfy the determinant, Eq.(4), but including the effect of 10% offset C.G. The numerical values of Fig.(8) do not apply to the CEGB conductor. The moment of inertia, r_a , for the CEGB conductor is about 56, 152 respectively. The mass relative density is about the same (~ 3000), and the offset C.G.(7%) is less. Further, the initial angle of attack appears too high for the bundle of four because of bundle stiffness. There is expected to be a large influence of initial angle of attack.

The above natural frequencies were computed by Tunstall and Koutselos for a twin bundled conductor. They are used here as a working tool to establish a certain realism for the analysis. However, later a more accurate estimate of the natural frequencies for the quad bundle is given.

It will be noted that the equations previously derived are quite general in scope, and can be applied to any number of sub-conductors - including a single- by an appropriate selection of frequency ratio (R), and mass radius of gyration squared, r_a (normalized on the diameter, d).

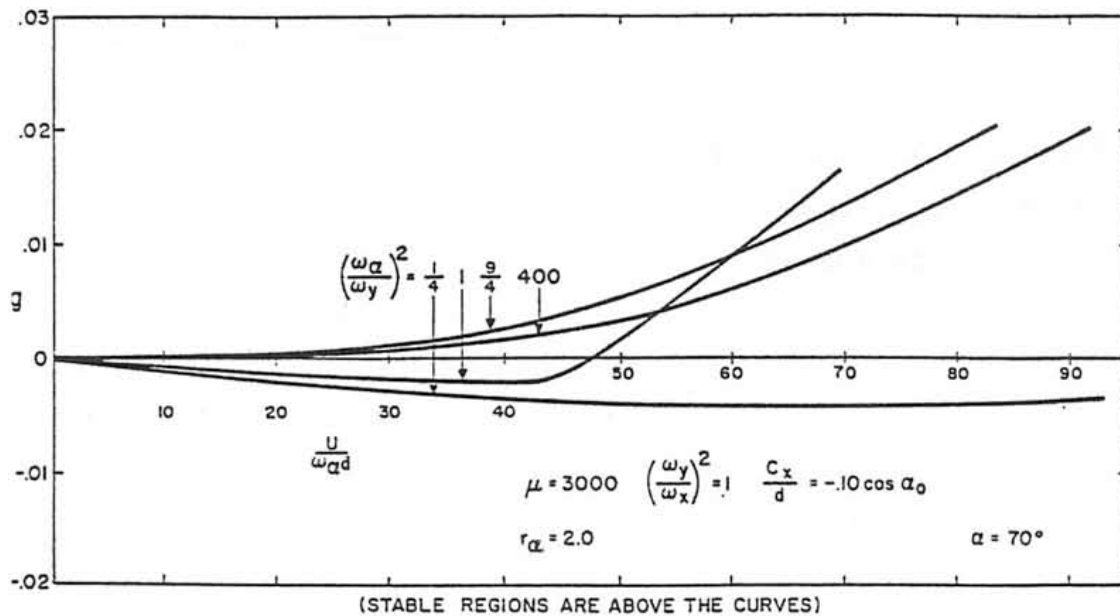


FIGURE 8
STABILITY BOUNDARIES FOR MODEL NO.2 FOR DIFFERENT $\left(\frac{\omega_\alpha}{\omega_y}\right)^2$ RATIOS
FROM THREE-DEGREE-OF-FREEDOM CALCULATIONS

A study was conducted, using Eq. (4) as basis, to determine the effect of the initial angle of attack. The results are seen in Fig. (9). The numerical values for the two curves are seen in Table 2.

TABLE 2. Numerical Values for Fig. (9)

Parameter	Curve Label (0)	Curve Label (z)
radius of gyration, r_a	56	152
gallop mode damping, g	300	200
torsion mode: μ ($R^2 - 1$)	248	248 (g=0)

The figure shows the reduced wind speed, U_0 , as abscissa, and the initial angle of attack as ordinate. Scales are respectively, 0-300, and 0-40 degrees. When the wind speed parameter exceeds the critical value, gallop occurs for the CEGB conductor. In the case of the .305m spaced bundle the critical wind is $U_0 = 70$, while for the 0.508m bundle it is $U_0 = 135$, almost double. In both cases, a significant benefit is available if the initial angle of attack is increased to 20 degrees or more. The critical wind speed values for the respective cases, and for the double loop gallop are: 4.66 m/sec and 8.99 m/sec. An initial angle of attack of only 20 degrees will almost double these figures.

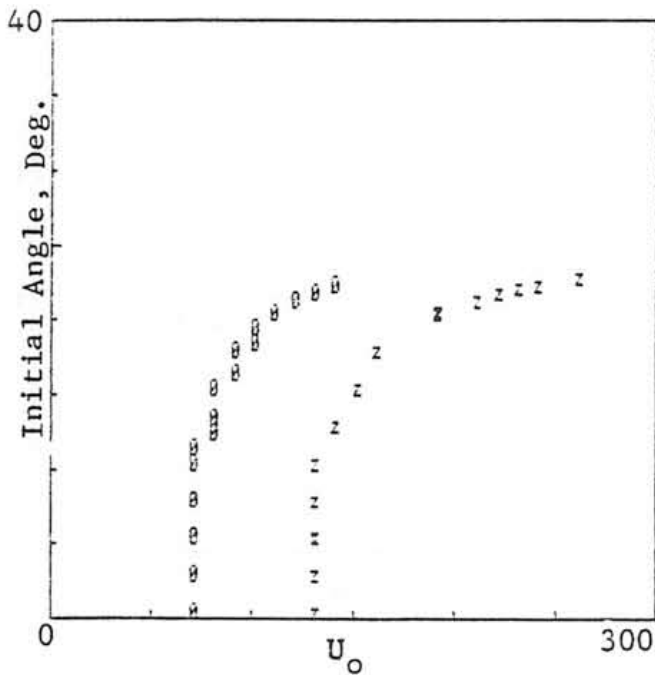


Fig.(9) Study of CEGB Quad Bundle
Curve labels, Table 2.
Effect of Initial Angle

The numerical values in Table 2 taken with Fig. (9) illustrate the favorable effect of the larger bundle. Also, the numerical value of mode damping in the gallop mode, though smaller in the case of the larger bundle, is offset by the favorable effect of large radius of gyration. These effects are present even though the frequencies are nearly matched. The numerical value of the torsion parameter μ (R^2-1)=248, translates into a frequency mismatch less than ten percent in both cases. Thus, while frequency ratio is important, it is not the only thing that is important. The damping ratio in the gallop mode is large by most standards. The g damping is just twice the damping ratio, so the numbers translate to a damping ratio of about 5%. It is apparent that damping of the gallop mode alone will not be completely effective. The initial angle of attack effect seems to work in both cases.

Offset C.G. Added:

Thus far, we have neglected the C.G. offset due to static unbalance of ice. If it is included, it is added to Equ. (3) on the diagonals of the matrix on left side of the equation. Inertia coupling terms equal to μE where E is the offset C.G. distance divided by the conductor diameter, or -0.07 in this case. The minus sign is used when the offset distance is on the windward side, and a plus sign is used when the offset distance is on the lee side of the conductor. When this effect is included in the equation, the effect of it is seen in Fig. (10), when the C.G. is on windward side. The curve label (0) is the same as the curve label (z) in Fig. (9), and apply to the conditions of the Table 2. The curve label (y) applies to the -0.07 offset. It is seen to increase the critical wind speed from $U_0=135$ to $U_0=200$.

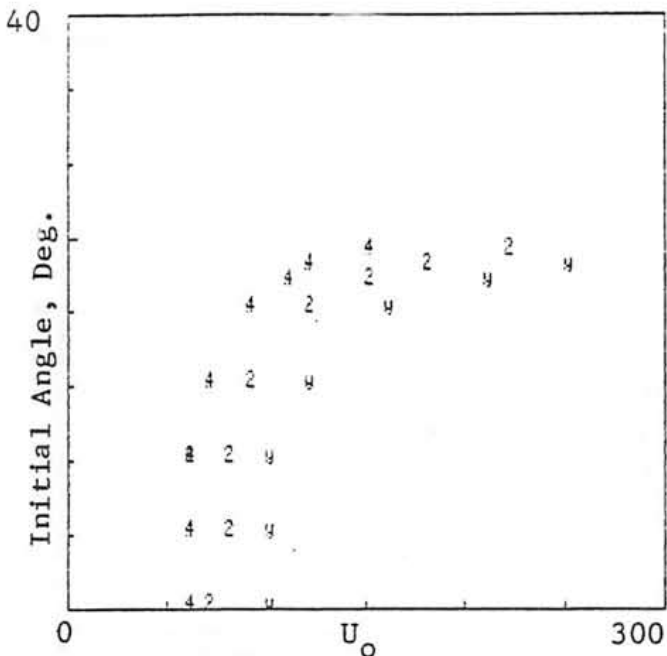


Fig. (11) C.G. AFT

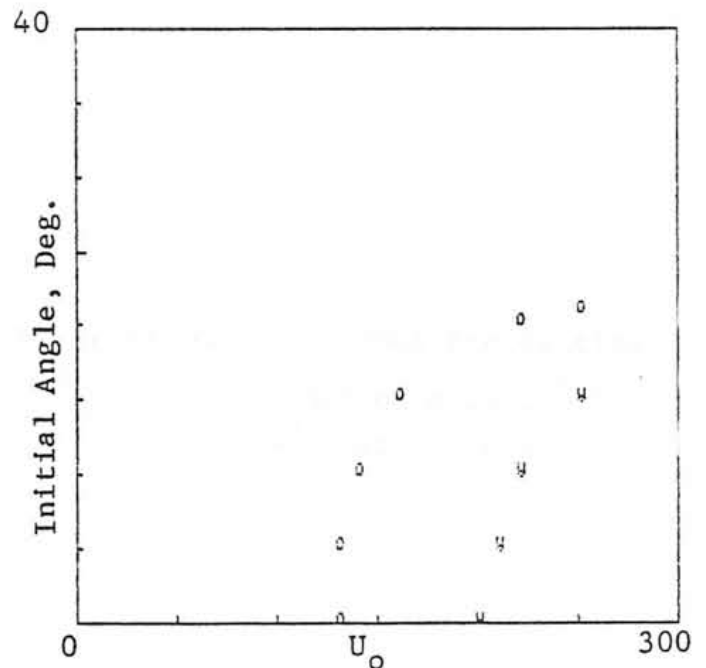


FIG. (10) C.G. FWD

It is of interest to compare these results with offset C.G. on the lee side of conductor. The results for that case are seen in Fig. (11), and again the conditions under the (z) label of Table 2 apply, except for the C.G. offset. The numerical values of C.G. offset in Fig. (11) are: $y=+0.07$, $z=+0.14$, & $4=+0.28$. Increasing the C.G. offset when it is positive reduces the critical speed, U_0 . Comparing the two figures, it is seen that the normal situation where ice accumulates on the leading edge, or windward side, is helpful. This is not the reason that unbundling of bundles is helpful, however. The reason that the wind-side offset C.G. helps is the same reason that a forward location of the center of gravity helps to prevent wing flutter in airplanes. It is the same reason that wing-mounted engines are mounted forward of the wing twist axis, rather than back of it. It is a well known strategy to the flutter analyst. However, in the case of a bundled conductor, there is no way that the strategy could be exploited because there is no way of adding offset weight that will always be to windward. Calculations which show the effect of offset C.G. are illustrated in Table 3. Again, the conditions of Table 2 apply.

TABLE 3 Effect of C.G. Offset

ra = 56		($\mu g_1=300$)	ra = 152	
U_0		μE	U_0	
130		-225	210	
200		-450	290	
>500		-675	>500	
70		+225	130	
60		+675	100	
50		+1000	90	
50		+2000	70	
50		+3000	70	

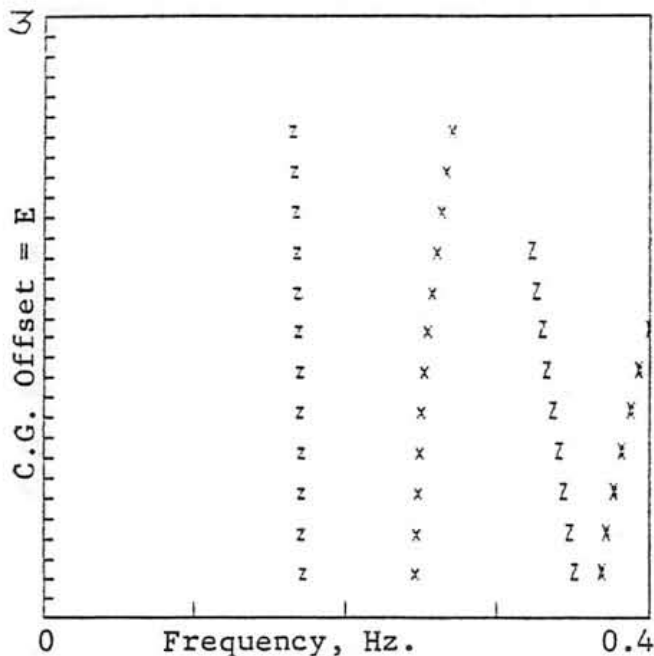


Fig. (12) Coupled Modes Frequencies

Z = Gallop motion
X = Twisting motion

Coupled Modes:

The idea of increasing the C.G. offset to the point that the two modes couple was examined. This was done by dropping all damping terms and aerodynamic terms from the equations (3), while retaining all inertial terms including the μE terms. The results of this study are seen in Figs. (12)-(14). The effect on mode frequency is seen in Fig. (12). The ordinate is μE on a scale of 0 to 3. The abscissa is modal natural frequency on a scale of 0 to 0.4 Hz. The z symbol is the 'gallop mode branch' while the x symbol is the 'twisting mode branch'. Notice that both first and second mode frequencies separate, or become detuned, as the offset inertia is increased. This is a well-known effect in dynamical systems that couple inertially. The spreading, or detuning is greater when the two frequencies are initially close together. Here the first mode has $R=1.4$, while the second mode has $R=1.044$. Figure (13) shows the eigenvector for the first coupled mode. The units are radians per unit diameter of the gallop mode displacement. The scale is, on the ordinate 0-3 units of μE , and 0-0.4 units of eigenvector, on the abscissa. The two branches gallop (z) and twisting (x) approach an asymptote equal to the inverse square root of ra . Here, we have taken $ra=56$. This asymptote is seen clearly in Fig. (14) for the second mode. The reason that the second modes couple more easily is because they were close to begin with. In either case, a large amount of inertia is required to bring the two modes together. An offset of two diameters of the bundle C.G. is about 30 times the offset associated with ice ($=0.07$).

Why would anyone want to introduce such a large offset, on purpose? With reference to Table 3, such a large offset will increase the critical wind speed only when the wind is on the same side as the offset. If it is on the opposite side, the critical wind speed is reduced, and there are few areas in the world that one could rely on the one-sided offset arrangement for protection against gallop. There is another reason why one would seriously consider a one-sided offset device for gallop control. That reason is to be explained later, after some fundamental ideas about non-linear aerodynamics are brought into the analysis.

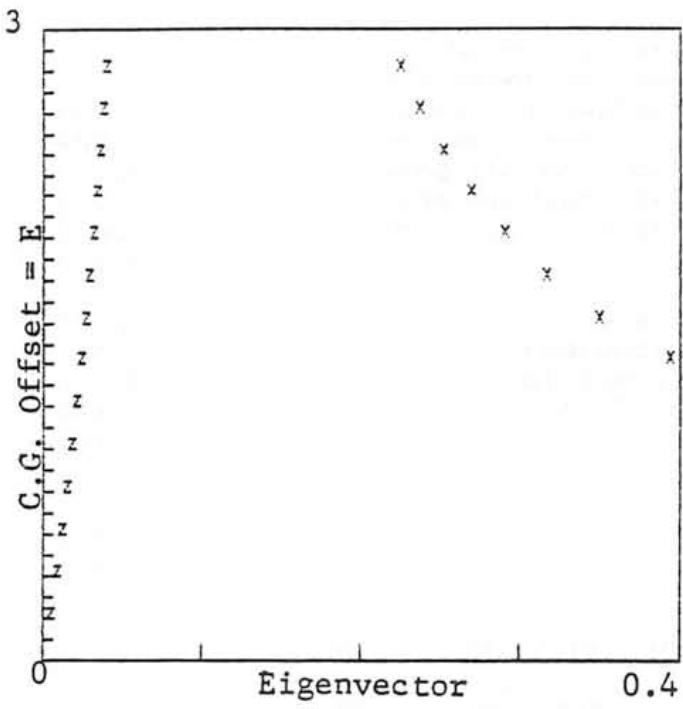


FIG. (13) Coupled Mode Eigenvector
First Mode

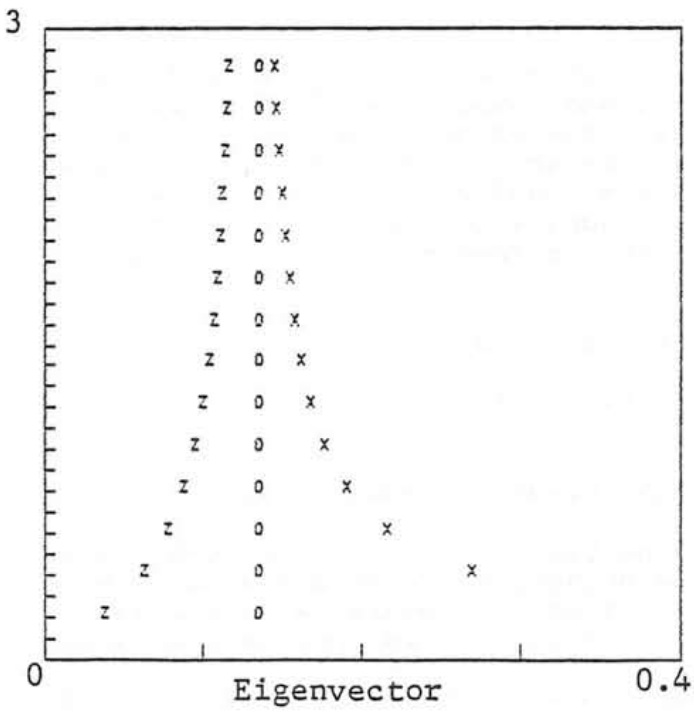


FIG. (14) Coupled Mode Eigenvector
Second Mode

Scale: Offset=E, 0-3
Eigenvector, 0-0.4
TOP: R=1.44, Bottom: R=1.044

Non-linear Analysis:

The previous analyses have indicated several conclusions: (i) large values of the radius gyration (moment of inertia) are desirable in terms of increasing the critical wind speed for gallop, (ii) initial angle of attack of the ice shape different from zero, and especially larger than 20 degrees, is desirable in terms of increasing the critical wind speed for gallop, (iii) increasing the C.G. offset in the windward direction is helpful to increase the critical wind speed of gallop, but increasing the C.G. offset in the lee direction is not helpful.

These trends are limited to the analysis of bundled cables, where, among other things the natural frequencies of gallop and twisting modes are close, and the moment of inertia of the system is more than 100 times larger than the moment of inertia of a single cable. Further, the analysis has included mostly aerodynamic coupling through the moment and lift coefficients. Inertial coupling has been identified, but little has been done about it, yet.

There is another interpretation that can be given to the equations of motion. The interpretation is as follows: (with reference to Eq.(3)).

$$Ar = [Uo / (\mu g + UoCD)] \times \tilde{CL}(Qo-Ar) \dots \dots \dots (6)$$

$$Qo = [Uo^2 / (\mu Dra)] \times \tilde{Cm}(Qo-Ar) \dots \dots \dots (7)$$

where,

- $\tilde{CL}(Qo-Ar)$ = Lift describing function
- $\tilde{Cm}(Qo-Ar)$ = Moment describing function
- $D = R^2 - 1$

Under the assumption that $R \sim 1$, pitch motion is in phase with the gallop velocity. As already noted, the pitch motion must ALWAYS generate forces in phase with gallop velocity when lift slope is positive. The functions, \tilde{CL} & \tilde{Cm} are the Describing Functions for the simple harmonic motion, Richardson, (1988) They are the equivalent Fourier series components for the lift and moment wave forms at the gallop frequency. Here, they are scalar quantities, for the particular lift and moment curves, they are found to be:

$$\tilde{CL}(z) = 1.3 J_1(\pi z) \dots \dots \dots (8)$$

$$\tilde{Cm}(z) = 1.4 J_1(1.15 \pi z) \dots \dots \dots (9)$$

The J_1 functions are the Bessel functions of the first kind, of order unity.

The above formulation is based on work already published, Richardson (1988), and employs a central assumption with regard to Eq.(3); namely, the drag coefficient is assumed constant over a cycle of vibration. Of course, the usual assumption that $R \sim 1$ applies. This is seen to be reasonable from Table 1.

The solution of the non-linear problem is found from Eq.(8) and (9) by subtracting Eq(6) from Eq.(7):

$$Z = F(Z) \dots \dots \dots (10)$$

and ,

$$Z = Qo - Ar$$

$$F(z) = [Uo^2 / (\mu Dra)] \times (1.4) \times J_1(1.15 \pi z) - [Uo / (\mu g + UoCD)] \times (1.3) \times J_1(\pi z)$$

The above formulation is for the case of zero initial angle of attack. When the initial angle of attack is not zero, the describing functions are no longer scalar quantities, but are vectors. However, only that part that is in phase with the gallop velocity is of interest. It has a diminished level owing to the phase shift of the lift or moment away from gallop velocity. The diminished level is accounted for by a cosine multiplier function:

For lift (initial angle= θ_0): $CSL = \cos(\pi \theta_0 z) \dots \dots \dots (11)$

For moment: $CSM = \cos(1.15 \pi \theta_0 z) \dots \dots \dots (12)$

The solution is illustrated in Fig. (15). The conditions are: curve x is for $U_0=200$, curve q is for $U_0=150$. The plot is $F(Z)$ and the straight line is Z . The scale is 0-1 on both abscissa and ordinate. The intersections are indicated by hexagonal boxes. These are the solution points for Z . Once a solution point is found, that is used in Eq. (6) to find the correct value for the reduced angle of attack, A_r . A set of solution points is seen in Fig. (16) for values of gallop mode damping, $\mu_g=300$; detuning parameter, $\mu_D = 150$, and for the radius of gyration (squared) = 56. The latter corresponds to the smaller quad spacer of Table 1. The lower curves are the reduced angle of attack, the upper are the pitch angle, Q_0 . The abscissa scale, U_0 , runs from 0 to 300, and the ordinate scale from 0 to 3 radians. Other values of the three principal parameters are seen in Figs. (17) through (19). The trend is the same as the linear analysis; namely, large moment of inertia is helpful, large pitch frequency is helpful. Finally, the effect of initial angle of attack is seen in Fig. (20). The conditions are: gallop damping, $\mu_g=300$, detuning parameter, $\mu_D=300$, $a = 56$. The curve labelled C is the pitch angle with zero initial angle, as is the curve labelled 'a', which is the reduced angle of attack. The curve labelled by 'A' is the reduced angle of attack vs. U_0 when the initial angle of attack is equal to ten degrees. The two curves labelled X, and x are respectively, the pitch angle, and the reduced angle of attack, when the initial angle of attack is equal to 25 degrees. The latter curves fall below 0.2 radians for all wind speeds considered.

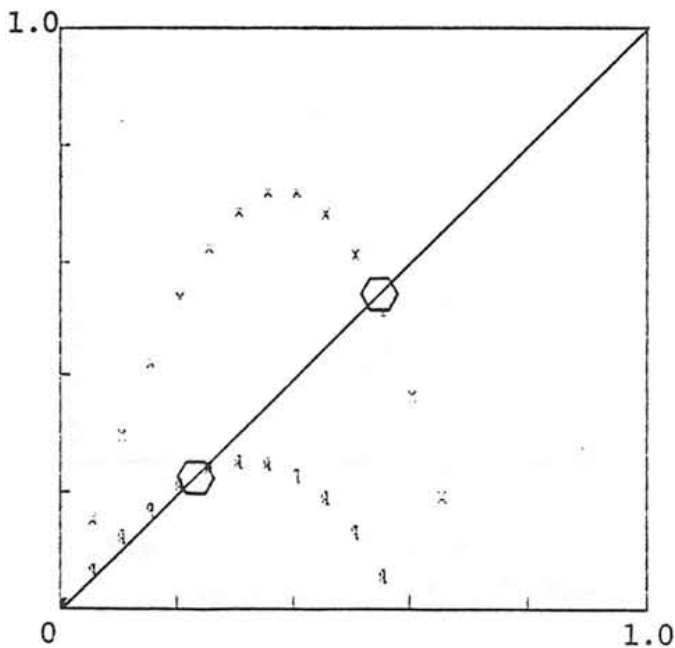


Fig. (15) Equ.(10) Solution

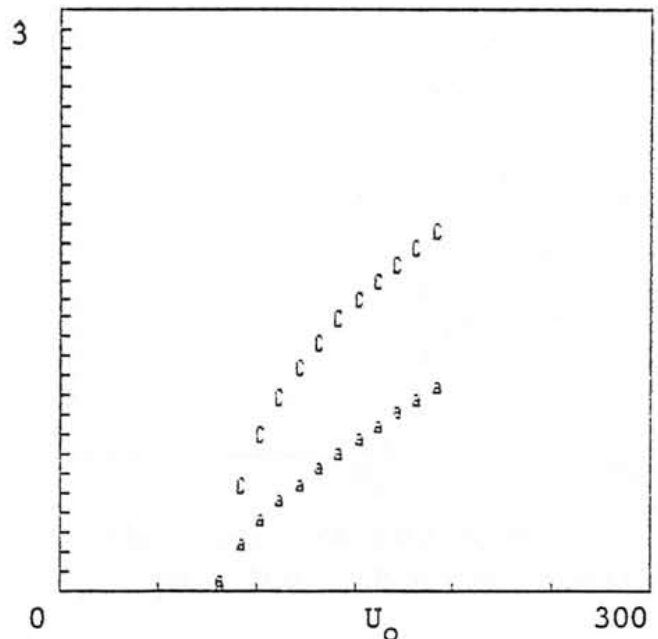


Fig. (16) Non-linear Gallop
 $\mu_g = 300, \mu_D = 150 \text{ ra}=56$

The effect of initial angle of attack in the non-linear analysis agrees with those trends found in the linear analysis; namely, large initial angle of attack is beneficial. Also, the trends from the non-linear analysis relating to the effect of radius of gyration agree with the trends from the linear analysis; namely, a large radius of gyration is beneficial. It is to be noted that the latter conclusion was found by Richardson and Martuccelli nearly thirty years ago, Richardson, (1965).

The effect of pitch frequency ratio may be separated from the effect of moment of inertia, by comparing Fig. (17) with Fig. (18), by comparing Fig. (18) with Fig. (16). It seems clear that the radius of gyration is more powerful than pitch frequency as to its effect on critical wind speed. Similarly, by comparing Fig. (18) and Fig. (19) it seems that gallop mode damping has little effect on critical wind speed, but it does diminish the gallop amplitude somewhat. However, as in the case of the linear analysis, the most dramatic reductions come from large effect of initial angle of attack. In particular, it is pointed out that the large reduction of gallop amplitude due to that effect pervades the wind speed range from very low critical wind speeds. This gives a clue concerning the use of large offset inertia as a control mechanism for bundle gallop.

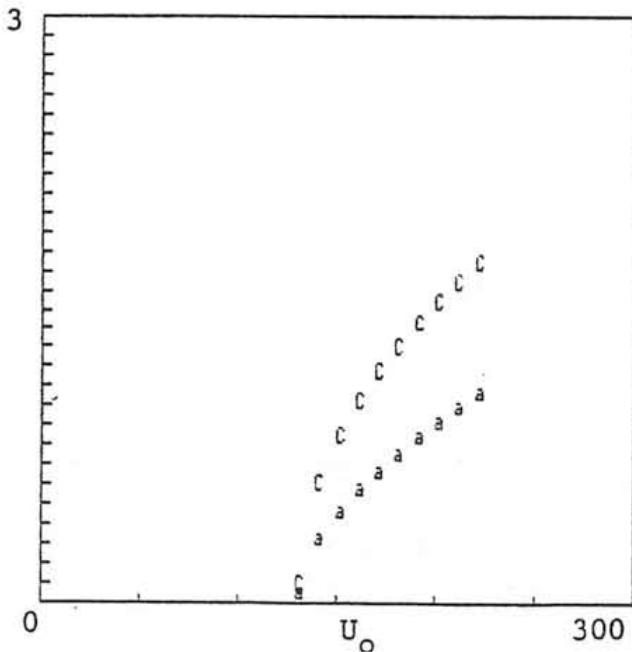


Fig. (17) Non-linear Gallop
 $\mu g = 300, \mu D = 300 \text{ ra}=56$

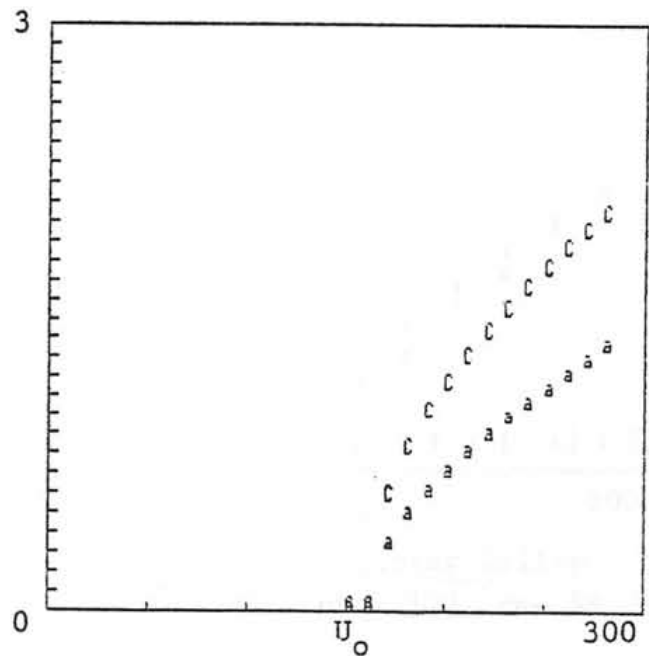


Fig. (18) Non-linear Gallop
 $\mu g = 300, \mu D = 150, \text{ ra}=152$

The detailed analysis of the large inertial unbalance must await another time. It is known from the coupled mode analysis that large 'doses' of inertial unbalance are at once beneficial and detrimental, depending on where the unbalance is with regard to the wind. The coupled mode eigenvectors are out of phase by 180 degrees, and either in phase or out of phase with regard to modal displacement. This means that the combinations of phasing that favor gallop - that is produce net lift forces in phase with gallop velocity - are limited to a finite range. Further, no coupled mode can gallop without twisting, and vice versa. Here are the ingredients for some clever design procedures that could increase the stability of the bundle. One thing that might be practical is to simply rotate the existing detuner pendulums on those lines that have galloped. A rotation of 90 degrees would produce a large inertial offset. If the offset is favored towards the wind side, so much the better. Another possibility is to hang weights on one side of the bundle that attach to the subconductors, both top and bottom. One should be careful not to add so much weight that the bundle would pre-twist to an undesired angle. These and other ideas require a detailed study to see if they might be practical.

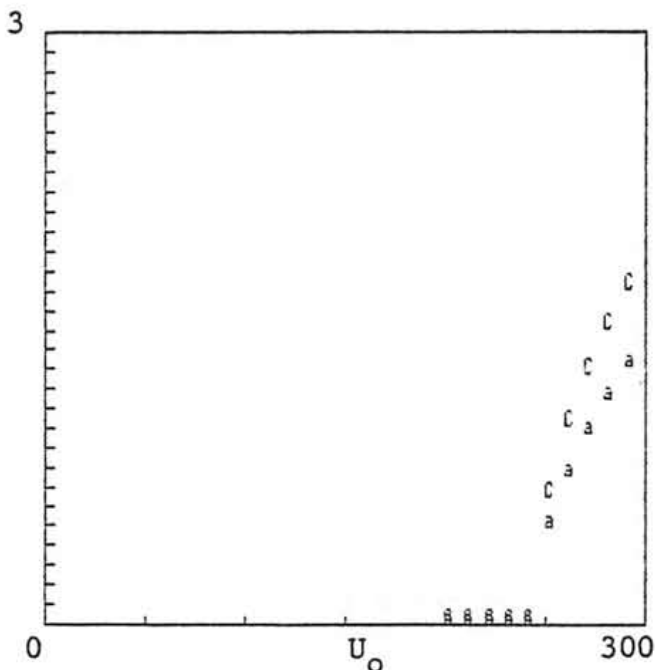


Fig. (19) Non-linear Gallop
 $\mu_g = 200, \quad u_D = 200 \quad r_a = 152$

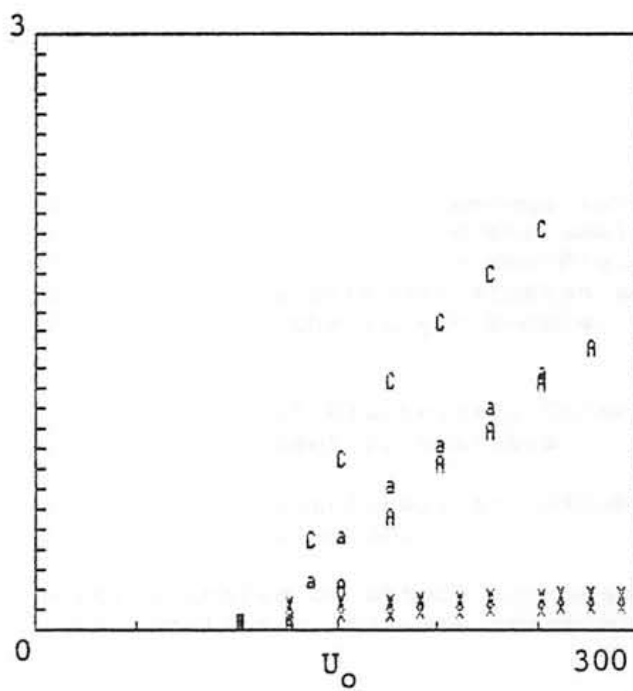


Fig. (20) Non-linear Gallop
 $\mu_g = 300 \quad \mu_D = 300 \quad r_a = 56$

Discussion:

The non-linear analysis gives results that are consistent with the linear analysis. In both cases, damping in the pitch mode has been neglected. In the non-linear analysis four effects are studied. The damping in the gallop mode has little effect on the critical wind speed. The radius of gyration in pitch of the bundle has a major stabilizing effect. Larger bundles give consistently higher critical wind speeds. The initial angle of attack, if large enough is capable of two important positive effects, (1) increasing the critical wind speed, and (2) reducing the amplitude of gallop. The bundle detuning has an observable effect. This last conclusion is supported by the range of detuning from 5 to 10 percent, (μD parameter from 150 to 300). The actual calculated natural frequencies, based on the larger spacer (0.508m) for the 355m span are: first mode gallop = 0.169Hz, first mode twisting = 0.178Hz, second mode gallop = 0.34Hz, second mode twisting = 0.362Hz.

In the larger bundle, if detuning pendulums are added to the bundle at spaced distances of 0.2, 0.33, 0.58, 0.75 along the span, then these frequencies are changed. The two gallop modes are unchanged, but the twisting frequencies become respectively: first mode = 0.25Hz ($R=1.4$) and second mode = 0.42Hz, and $R=1.23$. These calculations were based on an assumed cosine shape and an assumed sine shape respectively, along the span. Referring to Fig.(18), we see that the large bundle has been examined for relatively small detunings ($D=0.05$) and the finding has been favorable for the larger bundle. But, in the smaller bundle, the detunings are even greater by twice as much ($D=0.1$) - see Fig.(17). Yet, the critical wind speed is less. It appears that additional studies are required to separate the effect of higher detunings on the larger bundle.

CONCLUSIONS:

- o The gallop of a quad bundle based on an actual Central Electricity Generating Board (CEGB) transmission line has been studied by parametric analysis.
- o A linear analysis has shown that large bundles are less likely to gallop than small bundles. A non-linear analysis confirms that conclusion.
- o A linear analysis has shown that large initial angles of attack increases critical wind speed at which gallop begins. A non-linear analysis confirms that conclusion, and also indicates that large initial angles of attack reduce the gallop amplitude.
- o A small bundle with a high detuning ratio develops a lower critical wind speed than a larger bundle with a smaller detuning ratio. Detuning ratios are either 5% or 10%. Additional studies are required to sort out these effects.
- o A forward location of the C.G. is beneficial. An aft location is not. A study of the coupled modes resulting from very large offset C.G. devices may lead to new anti-gallop devices.

References:

- Chadha, J. A Dynamic Model Investigation of Conductor Galloping, IEEE conf. paper No. C 74 059 2, IEEE PES Winter meeeting, New York, NY, Feb., 1974.
- Lilien, J.L., Dubois, H., Overhead Line Vertical Galloping on Bundle Configurations, IEE Internationsl Conference on Overhead Line Design, Construction Theory and Practice, 28-30 November, 1988, Conf. Publ.# 297-65-69.
- Nakamura, Y., Galloping of Bundled Power Line Conductors, Jnl. Sound & Vibr., (1980) 73(3), 363-377.
- Richardson, A.S., Martuccelli, J.R., Price, W.S., Research Study on Galloping of Electric Power Transmission Lines, Paper 7, 1st symposium on Wind Effects on Buildings and Structures, Teddington, England, June 26-28, 1963, p.612.
- Richardson, A.S., Predicting Galloping Amplitudes, ASCE Journ. Eng. Mech. Div. Vol. 114, No. 11,, November 1988, p. 1945.
- Koutselos, L.T., Tunstall, M.J., Further Studies of the Galloping Instability of Natural Ice Accretions on Overhead Line Conductors, fourth Intl. conf. on Atmospheric Icing of Structures; Paris, 5-7 September, 1988
- Tunstall, M.J., Observations of Galloping and Control Method Performance on the CEGB System, Winters 1985/86 and 1986/87., CIGRE WG 22-11, rpt no. 87-17.